

# Injectable ROS-scavenging hydrogel with MSCs promoted the regeneration of damaged skeletal muscle

Journal of Tissue Engineering  
Volume 12: 1–15  
© The Author(s) 2021  
Article reuse guidelines:  
sagepub.com/journals-permissions  
DOI: 10.1177/20417314211031378  
journals.sagepub.com/home/tej



Huajian Shan<sup>1\*</sup>, Xiang Gao<sup>1\*</sup>, Mingchao Zhang<sup>1\*</sup>, Man Huang<sup>2</sup>,  
Xiyao Fang<sup>1</sup>, Hao Chen<sup>1</sup>, Bo Tian<sup>1</sup>, Chao Wang<sup>3</sup>, Chenyu Zhou<sup>4</sup>,  
Jinyu Bai<sup>1</sup> and Xiaozhong Zhou<sup>1</sup>

## Abstract

Skeletal muscle injury is a common disease accompanied by inflammation, and its treatment still faces many challenges. The local inflammatory microenvironment can be modulated by a novel ROS-scavenging hydrogel (Gel) we constructed. And MSCs could differentiate into myoblasts and contribute to muscle tissue homeostasis and regeneration. Here, Gel loaded with mesenchymal stem cells (MSCs) (Gel@MSCs) was developed for repairing the injured skeletal muscle. Results showed that the Gel improved the survivability and enhanced the proliferation of MSCs ( $\approx$ two-fold), and the Gel@MSCs inhibited the local inflammatory responses as it promoted polarization of M2 macrophages (increased from 5% to 17%), the mediator of the production of anti-inflammatory factors. Western blotting and qPCR revealed the Gel promoted the expression of proteins ( $\approx$ two-fold) and genes ( $\approx$ two to six-fold) related to myogenesis in MSCs. Histological assessment indicated that the Gel or MSCs promoted regeneration of skeletal muscle, and the efficacy was more significant at Gel@MSCs than MSCs alone. Finally, behavioral experiments confirmed that Gel@MSCs improved the motor function of injured mice. In short, the Gel@MSCs system we constructed presented a positive effect on reducing skeletal muscle damage and promoted skeletal muscle regeneration, which might be a novel treatment for such injuries.

## Keywords

ROS-scavenging hydrogels, MSCs, skeletal muscle, regeneration

Date received: 1 March 2021; accepted: 23 June 2021

## Introduction

Skeletal muscle injury is one of the most commonly occurring traumas in high-energy traffic accidents, acute or chronic peripheral arterial occlusion, surgical and plastic surgery situations, or contusions caused by sports.<sup>1,2</sup> Injured skeletal muscle is capable of regenerating, due to stem/satellite cells in a quiescent state become active and differentiate into myoblasts which would further engage in the myogenic differentiation and eventually fuse to form new myofibers.<sup>1</sup> Meanwhile, macrophages are also involved in the repair of skeletal muscle damage in the process of inflammation. During skeletal muscle regeneration, macrophages mount an inflammatory response while exerting trophic roles on mesenchymal stem cells.<sup>3</sup> Most of the skeletal muscle injuries underwent a smooth repair. Nevertheless, there is still a need of effective

<sup>1</sup>Department of Orthopedics, The Second Affiliated Hospital of Soochow University, Suzhou, Jiangsu, China

<sup>2</sup>Department of Oncology, Suzhou Dushuhu Public Hospital, Suzhou, Jiangsu, China

<sup>3</sup>Institute of Functional Nano & Soft Materials, Soochow University, Suzhou, Jiangsu, China

<sup>4</sup>Faculty of Clinical Medicine, Xuzhou Medical University, Xuzhou, Jiangsu, China

\*These authors contributed equally to this work.

### Corresponding authors:

Jinyu Bai, Department of Orthopedics, The Second Affiliated Hospital of Soochow University, 1055 Sanxiang Road, Suzhou, Jiangsu 215004, China.  
Email: baijy@suda.edu.cn

Xiaozhong Zhou, Department of Orthopedics, The Second Affiliated Hospital of Soochow University, 1055 Sanxiang Road, Suzhou, Jiangsu 215004, China.

Email: zhouxz@suda.edu.cn



treatment for severe skeletal muscle trauma.<sup>1</sup> Currently, different strategies have been developed to promote muscle repair and regeneration, such as surgery, physical therapy, biomaterials engineering, and cell therapy. However, clinical treatments are greatly limited in their ability to repair damaged skeletal muscles in terms of structure and function.<sup>4,5</sup> Developing novel methods and materials is still necessary for tissue regeneration in skeletal muscle injuries.<sup>1,5</sup>

Skeletal muscle injury is accompanied by inflammation, including various activated inflammatory cells, pro-inflammatory mediators, and high levels of reactive oxygen species (ROS).<sup>6,7</sup> Inflammatory response is involved in the healing process of injured muscle. However, excessive and long-term inflammatory response is not conducive to the repair of muscle. The imbalance between M1 and M2 macrophages is believed to be the cause of persistence inflammation and associated limits in tissue regeneration.<sup>8–10</sup> Regulating the inflammatory microenvironment of tissue is critical for the regeneration of damaged muscle.<sup>8,11</sup>

The recent development of advanced biomaterials including inorganic materials, organic polymers, and their composites has shown great promise for accelerating the regeneration of damaged tissues.<sup>5,8,12,13</sup> Our previous studies revealed that silk fibroin loaded with MSCs promoted wound healing by regulating the polarization of macrophages,<sup>13</sup> and the ROS-scavenging hydrogels containing rapamycin regulated the inflammatory microenvironment of degenerated intervertebral discs and enhanced the regeneration of degenerated intervertebral discs.<sup>12</sup> Here, an *in situ* ROS scavenging hydrogel containing MSCs was constructed, which could modulate the local inflammatory microenvironment and improve the myogenic differentiation ability of MSCs, thereby promoting the regeneration of skeletal muscle tissue. In addition, MSCs could regulate the immune response and anti-inflammation effects by the inhibition of activated macrophages and T cells.<sup>14,15</sup> After skeletal muscle injury, MSCs at the injured site can differentiate into myogenic cells and further form muscle fibers, a critical player in the repair of skeletal muscle after injury.<sup>3,16</sup> Moreover, the Gel we constructed removed ROS in the inflammatory microenvironment, further reducing the inflammatory responses.<sup>12</sup> We hypothesized that injectable Gel could be utilized to deliver MSCs locally upon implantation into skeletal muscle injury site. Under the ROS abundant environment, the scaffold consumed ROS and gradually degraded to release the MSCs which inhibited inflammation and promoted regeneration of damaged skeletal muscle. Thus, we hope to find a new strategy to promote tissue regeneration by inhibiting the inflammation in the skeletal muscle injuries.

## Experimental section

### Materials, cells, and animals

Cell Counting Kit-8 (CCK-8) and Cell-Light Edu Kit was obtained from RiboBio Co. (Guangzhou, China). All flow

cytometry staining antibodies were purchased from Biologend; Western blot, immunohistochemistry, and immunofluorescence antibody were purchased from Abcam, Cell signaling technology (CST) and Proteintech, LPS were provided by Sigma-Aldrich Chemicals (St. Louis, MO), and fetal bovine serum (FBS) was purchased from Invitrogen/Gibco. Others were purchased from Sigma-Aldrich, which were followed the manual properly.

Mouse peritoneal macrophages were extracted from C57/BL6 mice. The macrophage was cultured in Dulbecco's modified Eagle medium (DMEM, Gibco, Grand Island, NY, US) containing 10% FBS.

Six-week-old female C57/BL6 mice were used to isolate MSCs. The use of mice was approved by the animal ethics committee of Soochow University. To isolate MSCs, 6-week-old C57/BL6 mice were sacrificed by cervical dislocation and the femurs were dissected. Low-glucose DMEM, supplemented with 10% fetal bovine serum (FBS), 2 mM glutamine, 200 U/mL penicillin, and 200 mg/mL streptomycin (this medium is denoted DMEMc), was injected into the dissected bone to collect bone marrow cells. These cells were maintained in six-well plates for a few days. Adherent cells were detached with 0.25% trypsin, centrifuged, resuspended, and plated in culture bottles with DMEMc at 37°C and with 5% CO<sub>2</sub>. After continuous passaging to the third generation, flow cytometric analysis was performed for identification of the purity of MSCs.<sup>13</sup> The myogenic differentiation induction medium was DMEM/Ham's F12 containing 2% horse serum, 1% glutamine, 1 ng/mL basic fibroblast growth factor, and 0.4 µg/mL dexamethasone without antibiotics.

Female C57/BL6 mice (6–8 weeks) were purchased from Cavens biogel (SuZhou) model animal research Co. Ltd. Experiments were performed in adherence to Institutional Review Board from Soochow University and were in compliance with relevant ethical regulations.

### Hydrogels preparation

The ROS-responsive hydrogel was synthesized according to the previous protocol.<sup>12,13</sup> Gel was obtained by crosslinking poly(vinyl alcohol) (PVA) with a ROS-labile linker: *N*1-(4-boronobenzyl)-*N*3-(4-boronophenyl)-*N*1, *N*1, *N*3, *N*3-tetramethylpropane-1,3-diamine (TSPBA). In brief, *N*, *N*, *N*', *N*'-tetramethyl-1,3-propanediamine (0.1 g, 0.75 mmol) and 4-(bromomethyl) phenylboronic acid (0.5 g, 2.3 mmol) were mixed in dimethylformamide solvent (10 mL) under 60°C overnight. After the addition of tetrahydrofuran (THF; 100 mL), mixture was filtered, and washed with THF three times (3 mL × 20 mL). High purity of TSPBA (0.3 g, yield 70%) was collected after drying in vacuum overnight. PVA (72 kDa; 98% hydrolyzed; 5 g) was dissolved in deionized water (100 mL) after stirring at 90°C to acquire clear solution. TSPBA (5 weight % (wt%) in H<sub>2</sub>O, 2 mL) and PVA (5 wt% in H<sub>2</sub>O, 2 mL) were mixed to form hydrogel *in vitro* experiments. Predetermined amount of MSCs was added to the PVA

solution and then mixed with TSPBA by dual syringes to form Gel@MSCs in skeletal muscle.

### **Model of skeletal muscle injury and animal grouping**

All animal experiments were approved by the Animal Care and Experiment Committee of the Soochow University. Skeletal muscle injury was induced in female C57BL/6J mice (6–8 weeks) by unilateral femoral artery and vein ligation.<sup>2,8,17</sup> About 10 days after skeletal muscle injury, the injured sites (near the gastrocnemius muscle) were injected with 10,000 MSCs and/or 100  $\mu$ L Gel. Forty experimental mice were randomly divided into five groups as Group 1: Control, Group 2: Injured, Group 3: Injured + Gel, Group 4: Injured + MSCs, Group 5: Combine (Injured + Gel@MSCs).

### **Mice skeletal muscle fixation and histology processing**

Gastrocnemius were fixed in 4% v/v paraformaldehyde for 24 h. The sample was then dehydrated by gradient alcohol, washed, and embedded in paraffin to obtain four continuous sagittal sections which were approximately 3  $\mu$ m thick per section (four sections per sample); H&E and Safranin Masson staining were performed on the slide.

### **Immunohistochemistry**

Gastrocnemius paraffin sections were incubated in citrate buffer (pH=6.0; Servicebio, G1202) for antigen retrieval and then incubated in 3% hydrogen peroxide at room temperature for 25 min in the darkness. The sample was evenly covered with 3% bovine serum albumin (BSA) and blocked at room temperature for 30 min to prevent binding of nonspecific protein binding. The sections were incubated with the following primary antibody at 4°C overnight: Rabbit anti-MYOG antibody (Proteintech, 18943-1-AP), Rabbit anti-MYOD1 antibody (Abcam, ab1835). The corresponding secondary antibody (HRP marker) was added to cover the tissue and incubated for 50 min at room temperature. A 3,3'-diaminobenzidine was added for coloration and hematoxylin for nuclei counterstaining. Then the sections were dehydrated and sealed and digitally scanned by a slide scanner.

### **Flow cytometry**

Macrophage line RAW264.7 cells or mouse peritoneal macrophages were cultured in 24-well plate with DMEM medium containing 10% FBS, MSCs, and/or Gel were added onto the bottom surface of the inserts. Macrophages stimulated LPS (500 ng/mL) in specified time were washed once in cold PBS to prepare single cell

suspension, and stained by flow cytometry antibodies, F4/80-FITC, CD80-PE, and CD206-APC at room temperature without light for 1 h and flow cytometry (BD) was used for analysis.

Mice skeletal muscle was extracted to make single cell suspension. The cell suspension was stained with antibodies CD45-FITC, CD11b-APC, CD80-PE, and CD206-PE in darkness for 1 h at room temperature. Flow cytometry (BD) was used for analysis.

**Immunofluorescence staining.** MSCs treated with H<sub>2</sub>O<sub>2</sub> and/or Gel were cultured on cell slide in 24-well plate bottom with DMEM medium containing 10% FBS. MSCs on cell slide were fixed in 4% paraformaldehyde for at least 30 min at room temperature (RT) and then washed with PBS for 10 min at RT. Permeabilization and blocking were carried out simultaneously in PBS containing 15% FBS, 2% BSA, and 0.1% saponin (all Sigma-Aldrich, USA) for 30 min at RT. Cells were rinsed with PBS and incubated overnight at 4°C with primary antibodies diluted 1:100 in PBS containing 15% FBS and 2% BSA. Primary antibodies were Rabbit anti-MYOG (Proteintech, 18943-1-AP) and Rabbit anti-MYOD1 (Abcam, ab1835). Stained cells were then washed three times for 10 min each with PBS followed by secondary antibodies diluted 1:100 in PBS. Hoechst (Vector Laboratories, USA) for nuclear/DNA labeling was used at a 1:1000 dilution in PBS. Cells were washed three times for 10 min each and quantified in ProLong Gold (Vector Laboratories, USA) overnight at 4°C.

### **Enzyme-linked immunosorbent assays (ELISA)**

The concentrations of IL-1 $\beta$ , TNF $\alpha$ , IL-6, and IL-4 were measured from the culture medium using a commercial ELISA kit (eBioscience, San Diego, CA, USA and R&D Systems, Minneapolis, MN, USA) respectively according to the manufacturer's instructions.

**Edu (5-ethynyl-20-deoxyuridine) staining.** MSCs were seeded into six-well plates (at  $1 \times 10^5$  cells in each well) and were treated with H<sub>2</sub>O<sub>2</sub> (500  $\mu$ mol) and/or Gel in specified time. An Edu Apollo-567 assay kit (RiboBio, Guangzhou, China) was utilized to quantify cell proliferation. Briefly, cell nuclei were co-stained with Edu and DAPI for 3 h, visualized under a fluorescent microscope (Leica, DM 4000, Germany). Cells in each field of view were then counted and analyzed by the Photoshop software Edu (positive cells/nuclei).

**Cell metabolic activity.** According to the manufacturer's instructions, the proliferation of cells was assessed through the CCK-8 assay. MSCs treated by H<sub>2</sub>O<sub>2</sub> and/or Gel were seeded into 96-well tissue culture plates ( $5 \times 10^3$  cells per well). Following incubation for 72 h, the cell metabolic

activity was estimated by recording CCK-8's optical density (OD) at 550 nm using a microplate reader.

**Co-culture of macrophages with MSCs.** For the establishment of the co-culture system of mouse peritoneal macrophages with MSCs using the Transwell system, macrophages ( $5 \times 10^4$  cells/well) were pre-plated in 12-well plates and the Transwell chambers (0.4  $\mu$ m pore size, Corning, Lowell, MA, United States) were placed in six-well plates. Subsequently, MSCs ( $5 \times 10^4$  cells/well) suspended in RPMI 1640 complete medium were added on the top of each Transwell. Finally, the co-culture system was placed in an incubator for 3 days at 37°C with 5% CO<sub>2</sub>.

**Quantitative real-time PCR (qPCR).** RNA was isolated from MSCs. Total RNA extraction was carried out using Trizol according to the manufacturer's protocol. The amount of extracted total RNA was measured by UV spectrophotometer (ThermoFisher) at 260/280 nm wavelength, and then reversely transcribed. The detailed protocols for qPCR were previously described.<sup>18</sup> The qPCR was performed by the SYBR Premix Ex Taq™ kit under the ABI-7500 PCR system (Shanghai, China).<sup>13</sup> mRNA expression was quantified by 2<sup>- $\Delta\Delta$ Ct</sup> protocol with glyceraldehyde-3-phosphatedehydrogenase (GAPDH) as the internal control. The primer sequences used were as follows: Mouse GAPDH primers (internal control): forward primer 5'-AGGTCGGTGTGAACGGATTTG-3' and reverse primer 5'-GGGGTCGTTGATGGCAACA-3'; Mouse MYOG primers: forward primer 5'-GAGACATCCCCTATTTCTACCA-3' and reverse primer 5'-GCTCAGTCCGTCATAGCC-3'; Mouse MYOD1 primers: forward primer 5'-CGGGACATAGACTTGACAGGC-3' and reverse primer 5'-TCGAAACACGGGT-CATCATAGA-3'; Mouse PAX7 primers: forward primer 5'-TGGGGTCTTCATCAACGGTC-3' and reverse primer 5'-ATCGGCACAGAATCTTGGAGA-3'.

**Western blotting.** Western blotting assays were performed by well-established protocols as in our previous studies.<sup>12,19</sup> The total protein amount of samples was determined by the BCA protein kit. About 20  $\mu$ g proteins were used for each well. Then, proteins were separated by sodium dodecyl sulfate-polyacrylamide gel electrophoresis and transferred to polyvinylidene fluoride membranes (Immobilon-P; Millipore, MA). After incubation with the primary antibody T-Akt (Santa Cruz, Cat# sc-81434), p-Akt473 (CST, Cat# 4060S), T-S6 (CST, Cat# 2317S), p-S6 (CST, Cat# 4858S), IL-1 $\beta$  (CST, Cat# 12703S), IL-6 (CST, Cat# 12912T), TNF- $\alpha$  (CST, Cat# 11948S), and  $\beta$ -actin (ABclonal, Cat# AC026), followed by incubation with secondary antibody (BOSTER, Cat# BA1054). Chemiluminescence reagents (Proteintech, Cat# PK10001) were added to the membrane. The targeted protein bands were visualized on X-ray film. The total gray of the interested band was quantified by the Image J software.

**Rotarod test.** Motor performance and balance skills of mice were evaluated on an accelerating rotating rod. The rotarod speed accelerated from 10 to 60 rpm, time was fixed at 300 s. The time taken for each animal to maintain its balance while walking on top of the revolving rod was measured.<sup>20,21</sup>

**Inclined plane test.** The inclined plane test was used to assess the behavioral recovery of the hind limbs from motor disturbances. The test consisted of measuring the maximum angle at which mice could support its body weight on an inclined board measured in degrees (0°–90°). The board was covered with a rubber mat having 1 mm high ridges. The mice were placed facing downwards on an inclined plane, and the highest angle at which a mouse could maintain its hold for 5 s was recorded and described as the "capacity angle" for that animal. At each test session, three separate measurements were made for each mouse, and the mean of the five was considered a single score for that mouse.<sup>22,23</sup>

**Balance beam.** Fine motor coordination and balance of mice were assessed using the balance beam test. The beam (2 cm wide, 100 cm length) was raised 40 cm. The test essentially examines the ability of a mouse to remain upright and to walk on the relatively narrow and elevated beam to one of the platforms. During a single day of testing each mouse was given three 60 s trials with a minimum of 10 min between the trials. The average time of all three trials was taken as the score for each mouse. A test trial was given to familiarize the mouse with the beam. For each trial, the mouse was placed in the end of the beam facing one of the platforms and then released. Record the time when the mouse arrives at the other end. If a mouse remained on the beam for the entire trial, the maximum time of 60 s was given.<sup>23</sup>

**Statistical methods.** All numerical data were tested for normality with Shapiro-Wilk test. In case of normality and homogeneity of variance in all the data, data were described with mean  $\pm$  standard deviation, and differences in each variable among groups were analyzed by one-way analysis of variance (ANOVA). If there were significant difference in a certain variable, differences between every two groups were tested with the Student–Newman–Keuls test. A *p*-value < 0.05 was considered significant. GraphPad Prism software version 7.0 (GraphPad Software, Inc.) was used for all statistical analyses.

## Results

### Characterization of injectable gel systems

Here, an in situ-formed ROS-scavenging scaffold loaded with MSCs was constructed to offer a new strategy for modulating the local inflammatory microenvironment to promote skeletal muscle regeneration (Figure 1(a)). ROS-labile



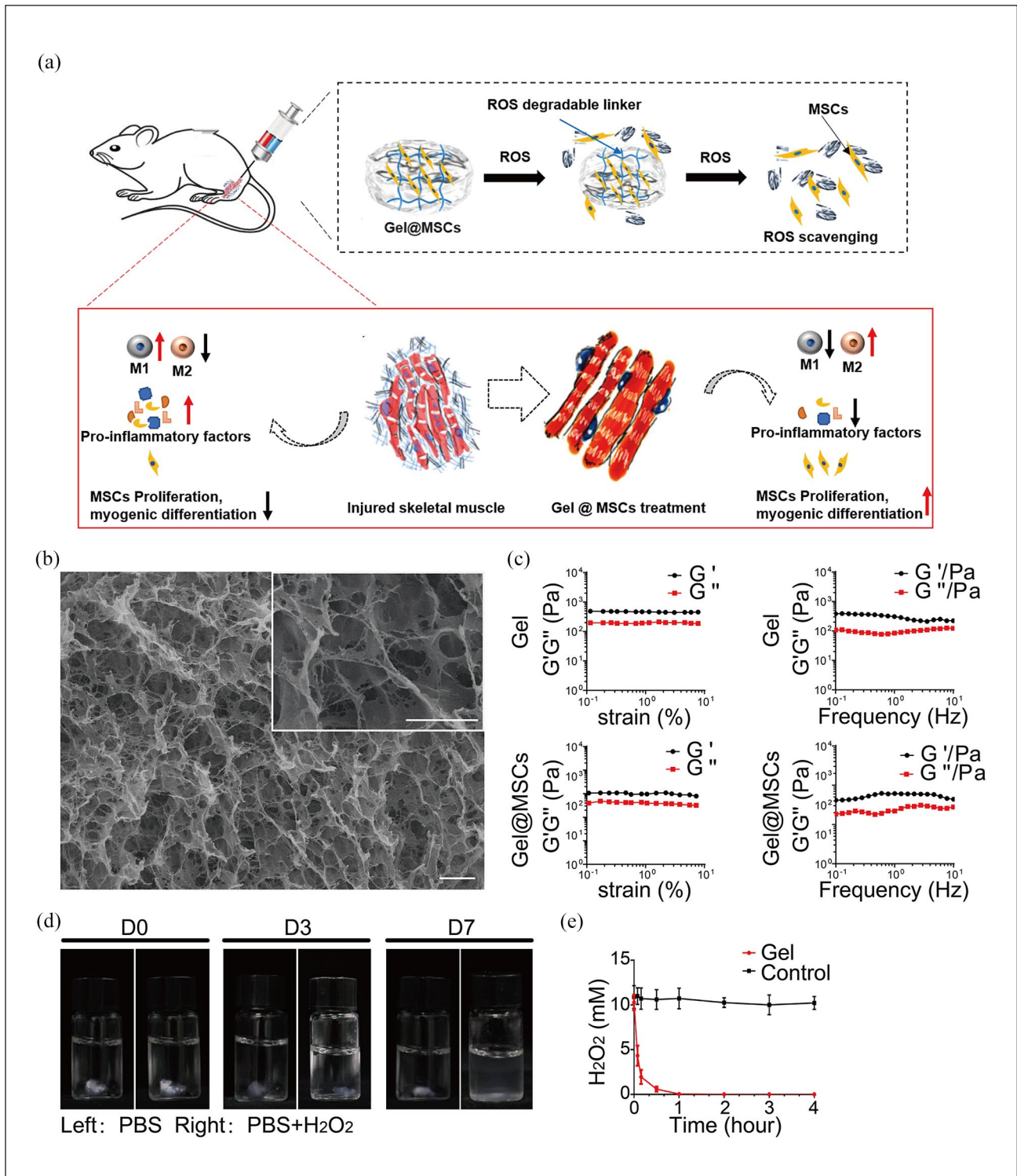


**Figure 1.** Schematic diagram and characterization of Gel. (a) Schematic diagram of Gel regulating skeletal muscle immune microenvironment and ameliorating tissue repair. Predetermined amount of MSCs was added to the PVA solution and then mixed with TSPBA by dual syringes to form Gel@MSCs in skeletal muscle. (b) Representative SEM image of gel scaffold. Scale bar, 2  $\mu\text{m}$ . Inset: enlarged image of the scaffold. Scale bar, 1  $\mu\text{m}$ . (c) The spectrum of elastic ( $G'$ ) and viscous ( $G''$ ) modulus of PVA-TSPBA and MSCs@PVA-TSPBA exhibited gel-like behavior. (d) Morphological changes of hydrogels in PBS with or without  $\text{H}_2\text{O}_2$  ( $1 \times 10^{-3} \text{ m}$ ) in 7 days. (e) Addition of PVA-TSPBA hydrogel to  $\text{H}_2\text{O}_2$  ( $20 \times 10^{-3} \text{ m}$ ), and evaluation of  $\text{H}_2\text{O}_2$  content by titanyl sulfate.

linker was synthesized *via* quaternization reaction of *N1,N1,N3,N3*-tetramethylpropane-1,3-diamine with an excess of 4-(bromomethyl) phenylboronic acid, and it was mixed with *N1*-(4-boronobenzyl)-*N3*-(4-boronophenyl)-*N1,N1,N3,N3*-tetramethylpropane-1,3-diamine (TSPBA). Gel was constructed by the crosslinking of two kinds of phenylboronic acids that could complex with diols of polyvinyl alcohol (PVA).<sup>24</sup> Porous structure of hydrogels network was shown by scanning electron microscopy (SEM; Figure 1(b)). Rheology test further indicated that the hydrogel was formed quickly after mixing PVA with ROS-labile linkers<sup>24</sup> (Figure 1(c)). MSCs were encapsulated in the hydrogel which did not affect the formation of hydrogel (Figure 1(c)). H<sub>2</sub>O<sub>2</sub> led to TSPBA oxidation and hydrolysis which induced degradation of scaffold and the release of payloads. The sample was then immersed in phosphate buffer solution (PBS) (pH=7.4) containing  $20 \times 10^{-3}$  mM H<sub>2</sub>O<sub>2</sub> at 37°C to observe morphology changes over time (Figure 1(d)). The level of H<sub>2</sub>O<sub>2</sub> in the solution was also detected by titanium oxysulfate.<sup>12</sup> Compared with the control group, H<sub>2</sub>O<sub>2</sub> in the surrounding environment was expended quickly during the degradation of hydrogel (Figure 1(e)).

Skeletal muscle injury accompanies ROS production, which could activate the pro-inflammatory signaling pathways by targeting major cellular macromolecules, including lipids, purine, pyrimidine bases, DNA deoxy-sugars, and amino acid residues.<sup>25</sup> Various strategies were used to inhibit inflammatory responses by ROS cleavage. We demonstrated that ROS-responsive/ROS-scavenging hydrogel scaffold effectively reduced the ROS *in vitro* (Figure 1(e)).

### ***ROS-scavenging hydrogels promoted the survival, growth, and proliferation of MSCs***

Skeletal muscle damage characterized by oxidative stress results from the imbalance between ROS induction and metabolism.<sup>26,27</sup> Many molecular signaling events characterize oxidative stress, including the production of hydrogen peroxide (H<sub>2</sub>O<sub>2</sub>), superoxide, and peroxynitrite.<sup>27,28</sup> H<sub>2</sub>O<sub>2</sub> (100 μM) was used to simulate MSCs damage under oxidative stress. H<sub>2</sub>O<sub>2</sub> inhibited the survival, growth, and proliferation of MSCs (Figure 2(a)–(d)). Nuclear EdU incorporation (% vs Hoechst) increased in MSCs when treated with Gel. Gel could alleviate the inhibition of H<sub>2</sub>O<sub>2</sub> on the proliferation of MSCs (Figure 2(a) and (b)). When testing cell metabolic activity with a CCK-8 assay, we found that Gel improve the metabolic activity of MSCs and reduce the influence of H<sub>2</sub>O<sub>2</sub> on the activity of MSCs (Figure 2(c)). Cells growth curve results demonstrated that the MSCs treated by Gel underwent a faster growth than control. In addition, Gel reversed the inhibitory effect of H<sub>2</sub>O<sub>2</sub> on the growth of MSCs (Figure 2(d)). To investigate whether the hydrogel systems in the present work would protect the implanted cells from death *in vivo*, the MSCs

were transfected with Luc<sup>+</sup>/GFP<sup>+</sup>.<sup>13</sup> The MSCs and Gel were injected into skeletal muscle tissue, and cell viability based on the bioluminescence was measured. As a control, no MSCs were found 7 days post injection in muscle tissue. In contrast, the hydrogels protected and stabilized the MSCs at the injection sites. After 7 days, the viable MSCs remained in muscle tissue for the Gel@MSCs groups, suggesting the superiority of the injectable hydrogels as MSC-laden systems (Figure 2(e)). The PI3K/Akt/mTOR pathway is an important signaling pathway that regulates cell growth and proliferation.<sup>29–31</sup> MSCs were treated with H<sub>2</sub>O<sub>2</sub> and/or Gel *in vitro*, and Western blotting was used to check the activation of PI3K/Akt/mTOR signals in MSCs. Results showed that p-Akt and p-S6 protein expression were reduced in MSCs treated by H<sub>2</sub>O<sub>2</sub>, while Gel increased the expression of p-Akt and p-S6 and even reversed the effect of H<sub>2</sub>O<sub>2</sub> on the expression of p-Akt and p-S6 (Figure 2(f) and (g)). These results confirmed that gel could reduce or even reverse the effect of inflammation on the activity and proliferation of MSCs by promoting PI3K/Akt/mTOR signaling pathway in MSCs.

### ***Gel, MSCs inhibited inflammation, and promoted M2-type polarization of macrophages***

Proinflammatory cytokines and polarization of M1 macrophages expression is known to increase when skeletal muscle tissue is damaged.<sup>6–8</sup> In addition, studies have reported that MSCs could reduce inflammation<sup>32,33</sup> and transform macrophages to an M2 immunophenotype.<sup>34</sup> Here, we studied the effects of ROS-scavenging hydrogels and MSCs on inflammation and macrophage polarization. To simulate the inflammatory immune microenvironment of injured skeletal muscle tissue, mice peritoneal macrophages cultivated in the lower part of the Transwell chamber were treated with lipopolysaccharide (LPS, 200 ng/mL), and Gel and/or MSCs were added to the upper level. ELISA, flow cytometry analysis, and Western blot were carried out after 24h (Figure 3). As expected, LPS-treated macrophages exhibited the typical M1 phenotype. Interestingly, the addition of Gel and/or MSCs into the LPS treated macrophages induced an increase of CD206 expression and a lower level of CD80 on macrophages. The combination of Gel and MSCs has the most significant effect, Gel and/or MSCs could inhibit the inflammatory response and M1-polarization induced by LPS, while enhancing the polarization of M2-like macrophages (Figure 3(a)–(c)). The expression of inflammatory factors (IL-1β, TNFα, IL-4, and IL-6) were detected through Western blot (Figure 3(d) and (e)) and ELISA assay (Figure 3(f)–(i)) as well. As expected, Gel or MSCs inhibited proinflammatory factor expression, and the inhibitory effect of Gel@MSCs was more obvious, which was consistent with the phenotype markers changes in the macrophages cells. We further investigated the modulating

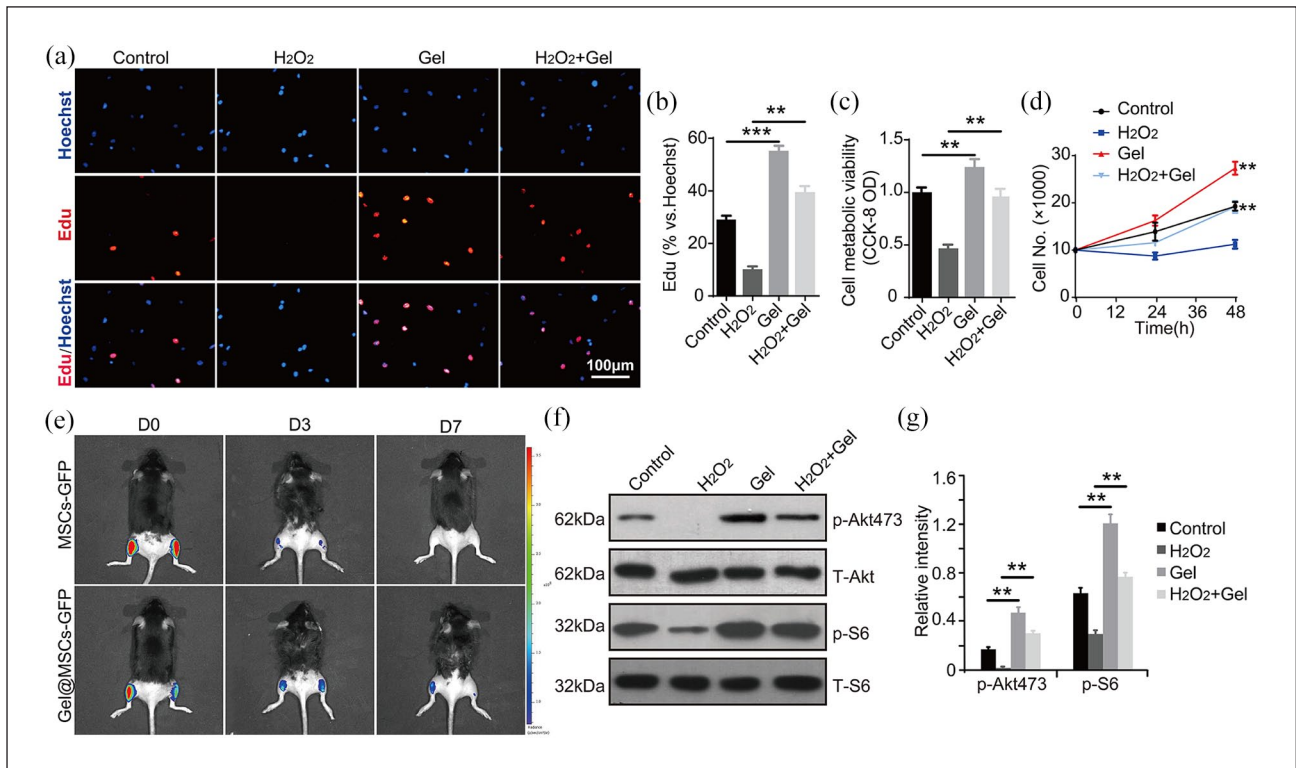


**Figure 2.** ROS-responsive hydrogel promoted the survival, growth, and proliferation of MSCs. (a–d) Cells were cultured for applied time periods, proliferation (nuclear EdU incorporation, A and B), MSCs metabolic activity (CCK-8 assays, (c)), and cell growth (d), were tested by the assays mentioned in the text, with results quantified. For Edu staining assays, five random views with total 1000 cell nuclei from each treatment were included to calculate the average Edu/DAPI ratio (same for all Figures). For all the cell functional assays the exact same number of viable cells of different treatments were seeded initially to each well or each dish (at 0 h/day-0, same for all Figures). (e) In vivo bioluminescence imaging of the GFP<sup>+</sup> MSCs in skeletal muscle when free cells, cell-laden Gel. (f) Expression of listed proteins was tested by western blotting. (g) Expression of listed proteins was quantified and normalized. Data were presented as mean  $\pm$  standard deviation (SD,  $n=5$ ). Experiments in this figure were repeated five times with similar results obtained. \*\* $p < 0.01$ , \*\*\* $p < 0.001$ .

effects of the Gel@MSCs on macrophage in vivo (Figure 4). Gel@MSCs was locally injected to the site on the third day after skeletal muscle injury. One week later, the tissues of mice skeletal muscle were extracted and make single cell suspension for flow cytometry analysis. Similar with the in vitro results (Figure 3(a)–(c)), tissue flow cytometry results showed that the expression of CD206 was upregulated while the CD80 was downregulated in Gel @ MSCs treated group (Figure 4(a)–(e)). The immunofluorescence results of CD80 and CD206 in skeletal muscle tissue were consistent with flow cytometry results (Figure 4(f) and (g)). These results suggested that Gel@MSCs could promote the polarization of macrophages towards M2-type in injured skeletal muscle tissue. In addition, separate injections of Gel or MSCs also had some effects.

### Gel promoted the myogenic differentiation of MSCs

Several transcription factors have been reported to have key regulatory roles in myogenesis of MSCs including

*MyoD*, *MYOG*, *PAX7*, and *MEF2*.<sup>35,36</sup> H<sub>2</sub>O<sub>2</sub> was used to simulate the inflammatory environment. MSCs were cultured in basic differentiation medium containing H<sub>2</sub>O<sub>2</sub> and/or Gel and in control medium without H<sub>2</sub>O<sub>2</sub> and Gel for 2 days. qPCR results showed that H<sub>2</sub>O<sub>2</sub> inhibited the expression of myogenic-related genes (*MYOD*, *MYOG*, *PAX7*, and *MEF2*) in MSCs, and Gel promoted the expression of myogenic-related genes, and reversed the inhibitory effect of H<sub>2</sub>O<sub>2</sub> on the myogenic differentiation of MSCs (Figure 5(a)–(d)). Immunofluorescence demonstrated that MYOD1 and MYOG were hardly expressed following H<sub>2</sub>O<sub>2</sub> stimulation in MSCs, while Gel induced the expression of MYOD1 and MYOG (Figure 5(e) and (f)). Immunohistochemical staining showed that MYOD1 and MYOG expression was upregulated in MSCs/Gel-treated group (Figure 5(g) and (h)). Western blotting showed that H<sub>2</sub>O<sub>2</sub> reduced expression of MYOD1 and MYOG, Gel increased the expression of MYOD1 and MYOG protein, similarly to the qPCR results (Figure 5(i) and (j)). The above results indicated that Gel promoted the myogenic differentiation of MSCs and reduced



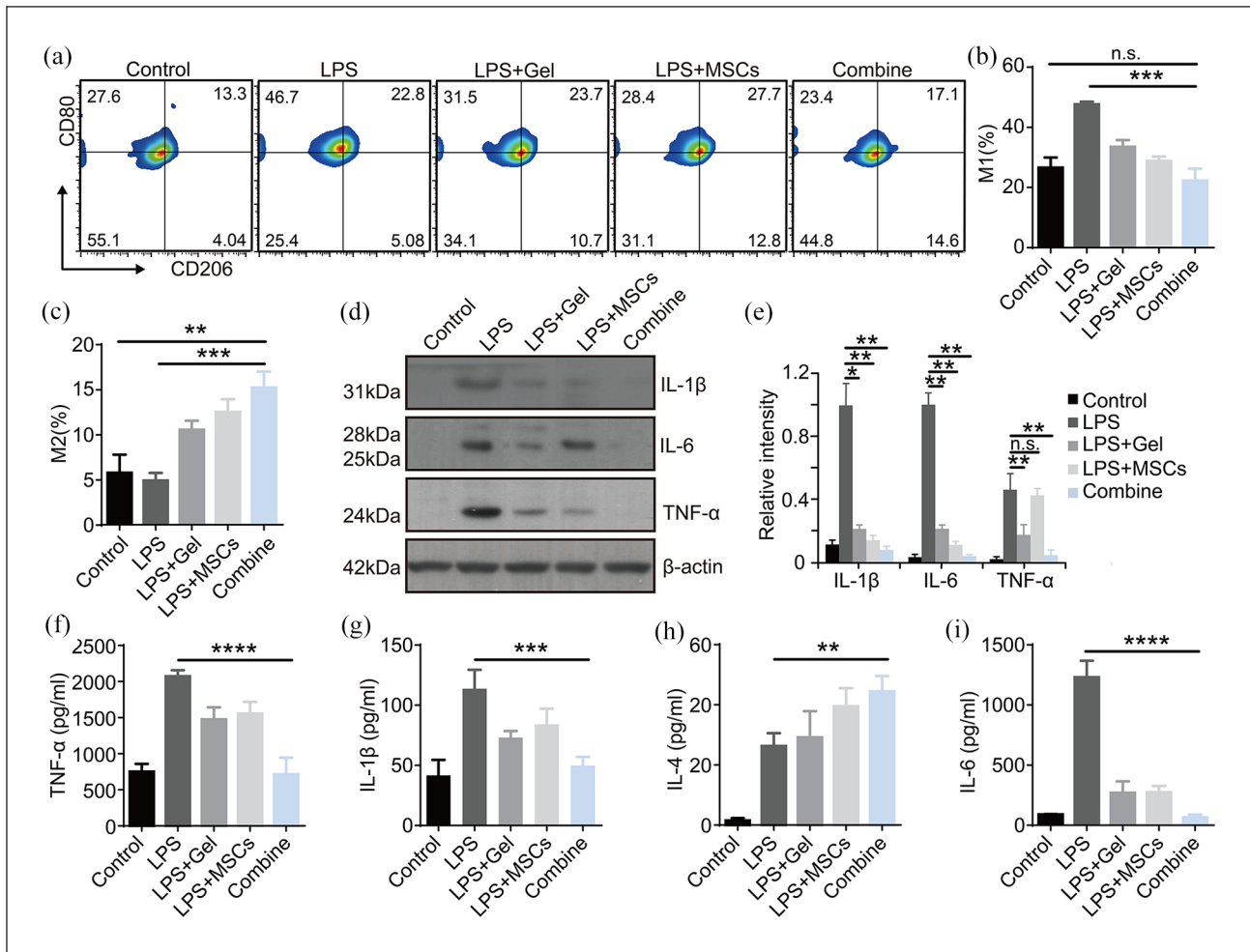


**Figure 3.** Gel@MSCs inhibited inflammation and promoted M2-type polarization of macrophages. Co-culture of Macrophages with MSCs, LPS (100 ng/mL) and/or Gel was added into mice peritoneal macrophages for 48 h. (a) Flow cytometry analysis was performed for the presence of CD80 and CD206 on the surface of macrophages. (b, c) Corresponding quantification results according to (a). (d, e) Western blotting data and corresponding quantification results showed the expression of listed proteins. (f–i) Levels of the proinflammatory cytokine TNF $\alpha$ , IL-1 $\beta$ , IL-6, anti-inflammatory cytokine IL-4, in mice peritoneal macrophages culture medium were measured by ELISA.

n.s.: nonsignificant.

Data were expressed as mean  $\pm$  SD ( $n=3-5$ ). Statistical significance was calculated by analysis of variance (ANOVA).

\* $p < 0.05$ . \*\* $p < 0.01$ . \*\*\* $p < 0.005$ . \*\*\*\* $p < 0.001$ .

the inhibitory effect of H<sub>2</sub>O<sub>2</sub> on myogenic differentiation. The combination of two had a better effect.

### *Gel and MSCs promoted the repair of damaged skeletal muscle and enhanced the recovery of motor function in mice*

To validate whether the proposed strategy could promote skeletal muscle regeneration, skeletal muscle injury was mimicked by ligating femoral artery and vein ligation (Supplemental Material Video). All the mice were randomly divided into five groups including control group, injured group, local injection of Gel group, local injection of MSCs group and Gel@MSCs treatment group. H&E and Masson staining were used to evaluate the regeneration of

skeletal muscle after various treatments (Figure 6(a) and (b)). H&E results also confirmed inflammatory cell infiltration, muscle fiber dissolution, fatty degeneration, and muscle tissue necrosis 10 days after injury. As we expected, local injection of Gel and MSCs into injured site reduced muscle damage (Figure 6(a)). Masson results showed that 10 days after skeletal muscle injury, the number of muscle fibers decreased and collagen fibers increased, which was not conducive to muscle function. Gel@MSCs reduced the formation of collagen fibers after being locally injected into the damage area on the third day after skeletal muscle injury (Figure 6(b)). After testing the effect of Gel@MSCs on mice motor function, we confirmed that Gel and/or MSCs did not affect the body weight of mice, but they reduced the weight loss after skeletal muscle injury, such



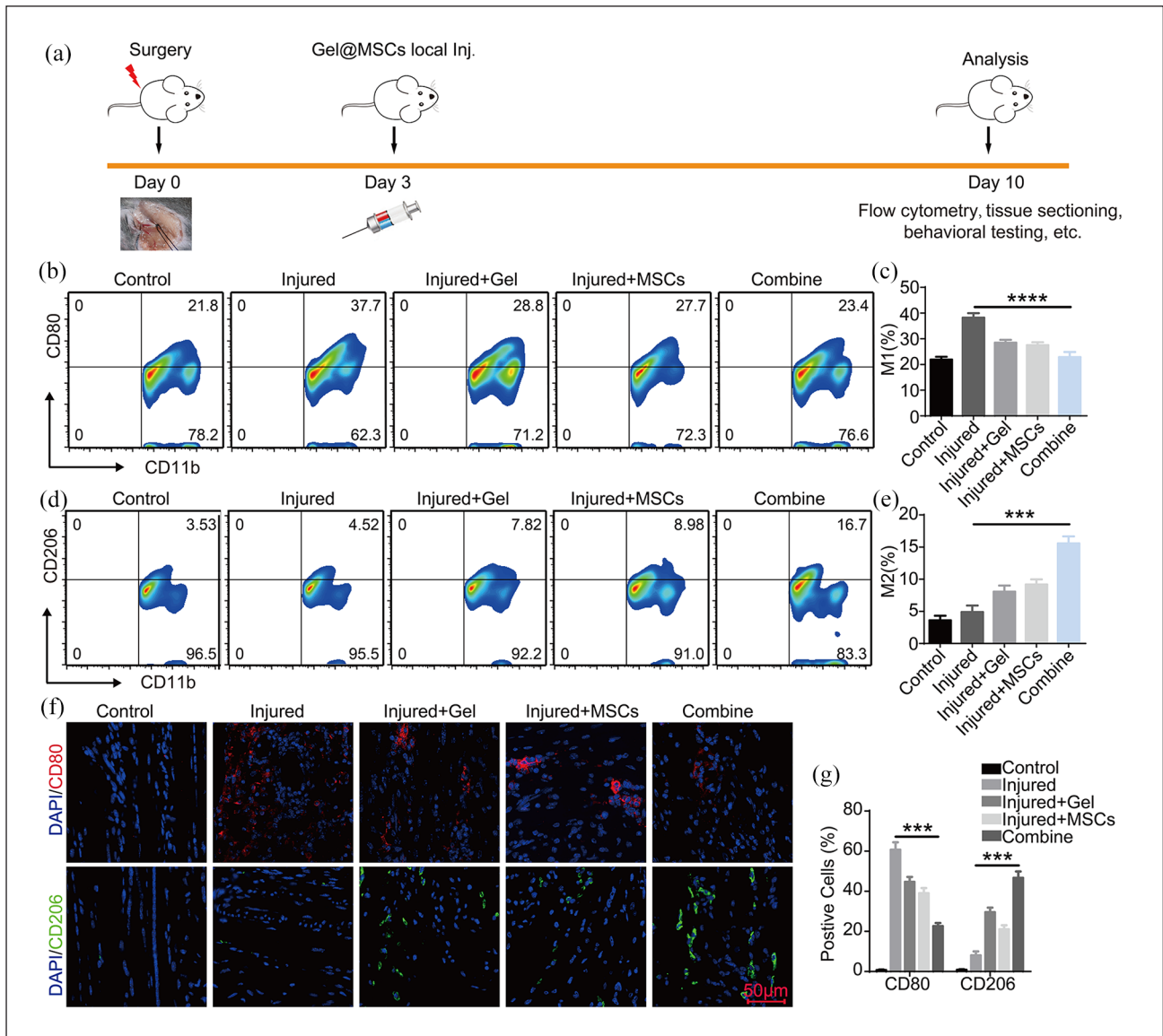


**Figure 4.** Gel@MSCs promoted M2-type polarization of macrophages in injured skeletal muscle. (a) Experimental design of mice skeletal muscle injury. (b, d) Injured skeletal muscle tissues were extracted from mice after various treatments as indicated after 10 days and expressions of CD11b and CD80, CD11b, and CD206 were determined by flow cytometry analysis. (c, e) Corresponding quantification results according to (b), (d). (f, g) CD206 and CD80 immunohistochemistry assay. n.s.: nonsignificant. Data were expressed as mean  $\pm$  SD ( $n=3-5$ ). Statistical significance was calculated by analysis of variance (ANOVA). Scale bars, 500  $\mu$ m. \*\*\* $p < 0.001$ . \*\*\*\* $p < 0.0001$ .

as gastrocnemius (Figure 6(c) and (d)). Mice motor functional was tested using the rotarod, inclined plane, and balance beam.<sup>21,37</sup> On one hand, mice with skeletal muscle injury needed to spend more time moving from one side of the balance beam to another side than the ones treated by Gel and/or MSCs (Figure 6(e)). On the other hand, the time of mice with skeletal muscle injury remaining on an accelerating rotarod was less than the mice treated by Gel and/or MSCs (Figure 6(f)). Tested by inclined plane, Grip strength of hind limbs decreased after skeletal muscle injury and this was reversed by Gel@MSCs (Figure 6(g)).

The above results confirmed that Gel and/or MSCs reduced skeletal muscle damage and promoted the recovery of skeletal muscle motor function.

#### Gel@MSCs were biological toxicity free to mice

Although biological toxicity of Gel was not observed in our previous work, we still systematically investigated the toxicology of Gel in mice over 1 week. To reveal any potential toxic effect of Gel on the treated mice, we carried out blood biochemistry and hematology analysis. Mice

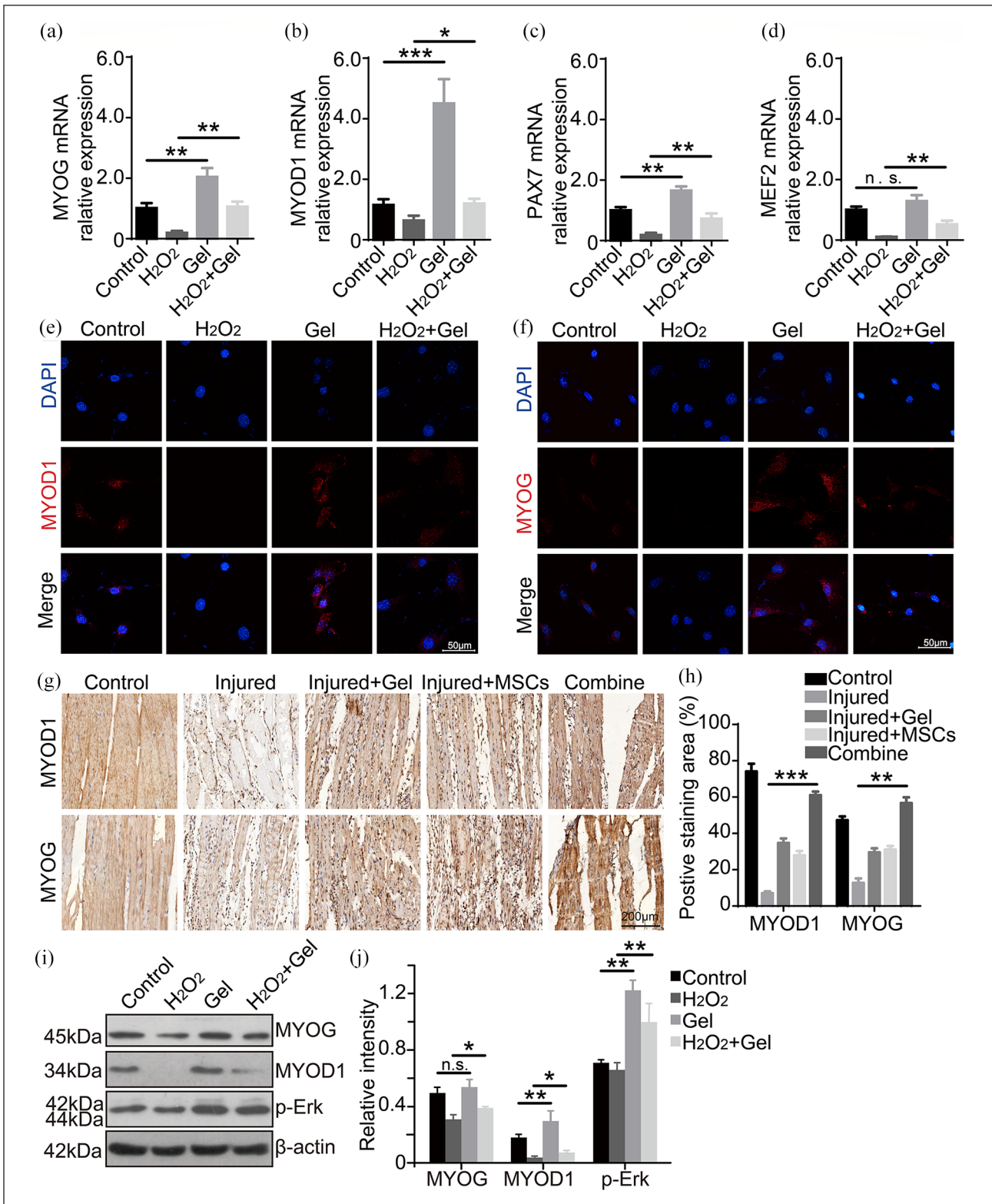


**Figure 5.** Gel promoted the differentiation of MSCs. (a–d) qPCR revealed the expression of key cytokine gene which induce myogenic differentiation from MSCs. (e, f) MYOD1, MYOG immunofluorescence assay. Blue color represents DAPI staining of nuclei. Red color represents MYOD1/MYOG. (g, h) Myogenic differentiation (MyoD1) and myogenin (MYOG) immunohistochemistry. (i, j) Western blotting data showed the expression of listed proteins.

n.s.: nonsignificant.

Data are expressed as the mean  $\pm$  SD ( $n = 3-5$ ). Statistical significance was calculated by analysis of variance (ANOVA).

\* $p < 0.05$ . \*\* $p < 0.01$ . \*\*\* $p < 0.001$ .

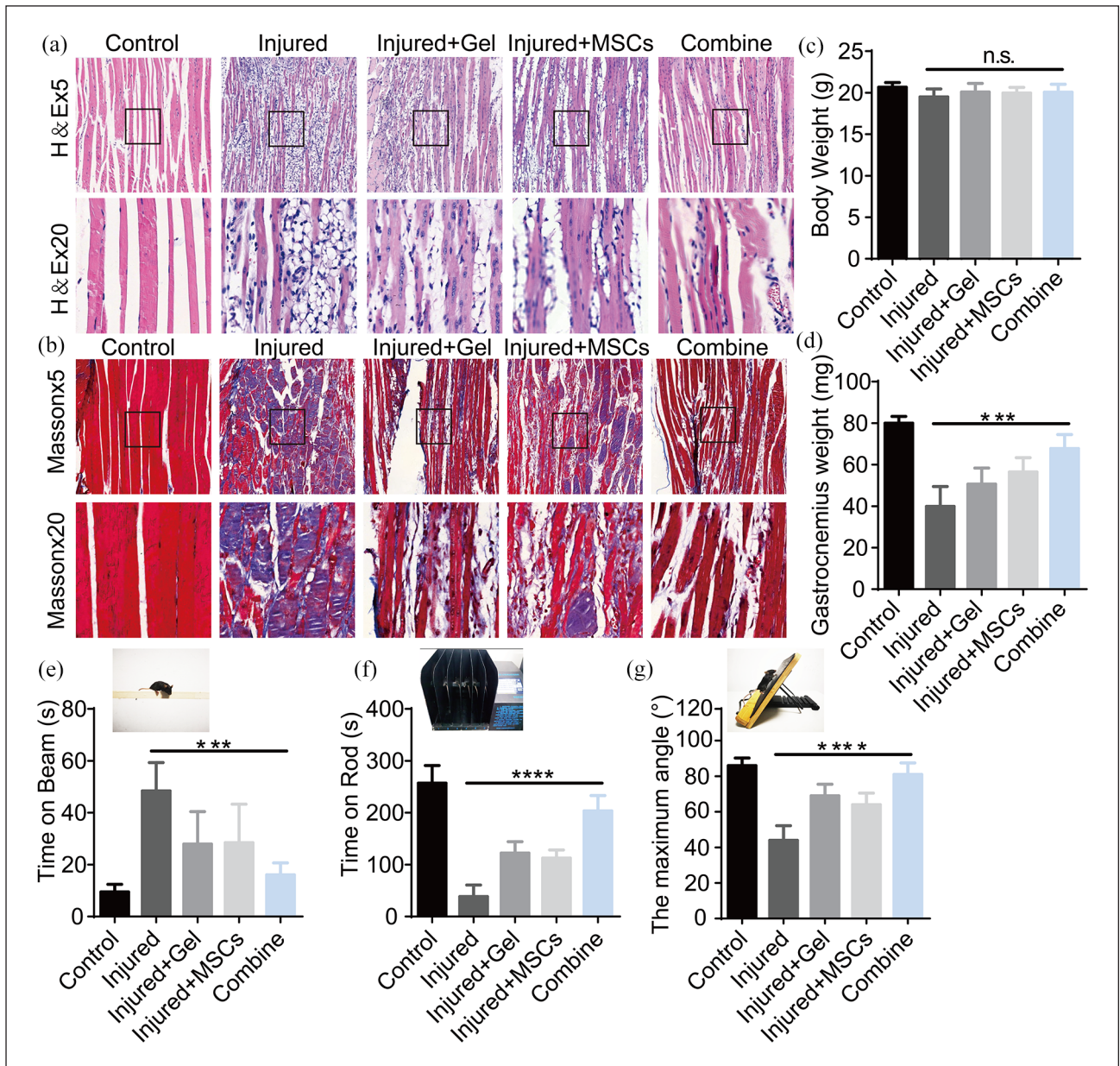


**Figure 6.** Gel@MSCs promoted the repair of damaged skeletal muscle and the recovery of motor function in mice. (a, b) H&E staining, Masson staining of experimental group and control group. (c, d) The mice body and gastrocnemius weights were recorded at 10th days of experiment. (e–g) Motion functional deficits assessed by balance beam, rotarod, and inclined plane test ( $n=6$ ). n.s.: nonsignificant. \*\*\* $p < 0.005$ . \*\*\*\* $p < 0.0001$ .

were sacrificed at 7 days p.i. for blood collection (five mice per group). Various biochemical indicators and hepatic or kidney function index including acid aminotransferase (ALT), aspartate aminotransferase (AST), glutamyltranspeptidase ( $\gamma$ -GT), alkaline phosphatase (ALP), and creatinine were measured. Compared with the control group, ALT, AST, ALP, and  $\gamma$ -GT had no significant change in Gel and/or MSCs treatment group (Supplemental Figure 1(a)–(d)). As the indicator of kidney functions, blood urea nitrogen (BUN) and creatinine levels

of injured mice increased (Supplemental Figure 1(e) and (f)), which may be caused by muscle fiber dissolution. Gel did not further increase BUN and creatinine levels, and even decrease their levels (Supplemental Figure 1(e) and (f)). Inflammatory cells in the blood of mice were evaluated. The percentage of lymphocytes and neutrophils in injured mice was significantly increased (Supplemental Figure 2(a) and (b)). Gel/MSCs could alleviate this phenomenon. In addition, our treatment strategy had no significant effect on monocytes (Supplemental Figure 2(c)).



Careful necropsy was conducted 7 days after injection of Gel and/or MSCs, and H&E staining showed that Gel and/or MSCs would not cause significant side effects on the heart, liver, spleen, lung, and kidney (Supplemental Figure 3(a)). The results above indicated that Gel would not cause any biological toxicity in mice, and could even reduce the increase in lymphocytes, BUN, and creatinine caused by skeletal muscle damage.

## Discussion

The data presented here illustrated that the hydrogel consisted of ROS-sensitive moiety loaded MSCs could accelerate regeneration and restore motor function of injured skeletal muscle by inhibiting inflammation, and promoting MSCs proliferation and myogenic differentiation. Previous reports showed that local transplantation of MSCs is beneficial to the repair of skeletal muscle injury,<sup>38,39</sup> while excessive and long-term inflammatory response at the injury site inhibit the myogenic differentiation of MSCs and the repair of damaged skeletal muscle.<sup>8,40</sup> How to regulate the inflammatory environment at the injury site to further promoting myogenesis of MSCs has always been one of the problems of skeletal muscle regeneration. Here, we found that MSCs and the Gel we designed could regulate inflammation, in particular the polarization state of macrophages. The combined use of Gel and MSCs was more effective. At the same time, Gel promoted MSCs proliferation and myogenic differentiation. Our data demonstrated that both inflammation and the polarization of macrophages (M2-type) in injured skeletal muscle could be regulated by our MSCs-loaded ROS-scavenging scaffold, which then enhanced the regeneration of damaged tissue and promoted the recovery of skeletal muscle motor function.

Acute skeletal muscle injury was accompanied by severe inflammation and high level ROS production.<sup>2,6</sup> This led to a massive influx of extracellular calcium and the activation of calcium-dependent proteases and phospholipases, which ultimately led to calcium-dependent necrosis, degeneration, and/or destruction of myofibrils.<sup>41–43</sup> In the context of inflammation, macrophages was one of the primarily responsible factors for the inflammatory response at the site of the muscle injury.<sup>6,44</sup> Various strategies were used to regulate the polarization of macrophages and inhibit ROS production in order to inhibit inflammatory responses.<sup>13,45,46</sup> Studies reported that MSCs could reduce inflammation<sup>32,33</sup> and promote polarize macrophages to an M2 immunophenotype via paracrine mechanisms.<sup>34</sup> However, biomaterials that could reduce skeletal muscle damage by removing ROS are very rare. Here, Gel we built and MSCs could be utilized to reduce the ROS, inhibit the production of inflammatory factors, and promote polarization of M2 macrophages. Our data showed that the Gel could inhibit LPS-induced inflammation, especially the expression of proinflammatory cytokines

and polarization of M1 macrophages. The combination use of ROS-responsive hydrogel and MSCs significantly inhibited the production of pro-inflammatory factors and the M1 polarization of macrophages in vivo and in vitro.

MSCs could differentiate into different type cells, such as myoblasts, osteoblasts, chondrocytes.<sup>47</sup> Hence, MSCs were used for the treatment of many diseases, including skeletal muscle injury.<sup>38,39</sup> Although MSCs have high-quality proliferation ability, studies have reported that transplanted MSCs showed poor tissue-specific differentiation ability.<sup>47–49</sup> In the environment of inflammation, excessive ROS impaired differentiation capacity and proliferation of MSCs.<sup>40,50</sup> Therefore, inhibition of the inflammatory response of damaged tissues is important to restore the function of MSCs. We showed that Gel was able to restore MSCs proliferation and myogenic differentiation in inflammatory microenvironment. At the same time, PI3K/Akt/mTOR pathway is an important signaling pathway that regulates cell growth and proliferation.<sup>29–31</sup> We found oxidative stress inhibited the phosphorylation of Akt473 and S6 in MSCs, while Gel promoted MSCs growth and proliferation by mediating the phosphorylation of Akt473 and S6. MAPK pathway with the Erk1/2 cascade is activated by various stimuli and contributes to regulate the differentiation of stem cells.<sup>51–53</sup> It's suggested that H<sub>2</sub>O<sub>2</sub> inhibited the phosphorylation of Erk, and the Gel promoted the phosphorylation of Erk1/2 in MSCs. At the same time, Gel promoted the expression of myogenic-related proteins (MYOD and MYOG) and genes (*MYOD*, *MYOG*, *PAX7*, and *MEF2*). So far, we confirmed that Gel enhanced MSCs proliferation and myogenesis via PI3K/Akt/mTOR and MAPK-Erk1/2 pathway.

Controlling the inflammatory response of damaged tissues could effectively inhibit subsequent damage and even promote tissues regeneration and repair.<sup>12,54</sup> Skeletal muscle regeneration is also regulated by inflammation.<sup>54</sup> After skeletal muscle injury, the muscle tissue underwent steatosis, necrosis, and fibrosis. Injection of Gel and/or MSCs into damaged skeletal muscle could inhibit the occurrence of these pathological processes. At the same time, the injections seem to promote the formation of new muscle fibers, which are important in inflammatory response and myogenic differentiation of MSCs in skeletal muscle tissue. Although different strategies have been used to promote skeletal muscle regeneration, the effects of these strategies on motor function after skeletal muscle injury are rarely studied.<sup>38,39</sup> We confirmed that after the skeletal muscles of the hind limbs of mice were injured, the motor function of mice was significantly impaired. Exogenous injection of Gel and/or MSCs could promote the recovery of mouse motor function, in improve performance in inclined plane test, balance beam inspection, and rotarod test. In addition, body weight of the mice had no change after hind limbs of mice were injured, but the weight of gastrocnemius muscle decreased. Our strategy could restore the weight of mice gastrocnemius muscle.



At the same time, we confirmed that our treatment system had no obvious toxic effects on the heart, liver, spleen, lungs, and kidneys based on results from their H&E, level of total IgG and lymphocytes in the blood. The above results made this strategy more clinically relevant for the treatment of skeletal muscle injury. In future studies, long-term toxicity of Gel@MSCs should be evaluated thoroughly for further translation to clinical application. Studies have reported that though MSCs had the role of myogenic differentiation,<sup>47</sup> there was the risk of tumorigenesis.<sup>55</sup> We would further study the tumorigenicity and optimize myogenic differentiation ability of MSCs.

In short, the system we had developed could regulate the local inflammatory microenvironment of damaged skeletal muscle, promote the regeneration of skeletal muscle and restore motor function of mice. Previous studies have shown that MSCs at the injury site would be damaged by the inflammatory factors.<sup>40</sup> The uniqueness of Gel@MSCs is that the Gel can not only regulate the inflammatory environment at the injury site, but also improve the survival and myogenic differentiation ability of MSCs. We found that the Gel and MSCs could reduce proinflammatory cytokines and enhance the polarization of macrophages to M2 type, which was anti-inflammatory and tissue-repairing macrophage that was important for promoting tissue repair. At the same time, MSCs in the presence of Gel could effectively differentiate myogenesis, and ultimately promote the recovery of skeletal muscle motor function.

### Author contributions

Huajian Shan, Xiang Gao, and Mingchao Zhang contributed equally to this manuscript. Jinyu Bai and Xiaozhong Zhou designed the project. Huajian Shan, Mingchao Zhang, and Xiang Gao performed the experiments and collected the data. All authors analyzed and interpreted the data, contributed to the writing of the manuscript, discussed the results and implications, and edited the manuscript at all stages.

### Declaration of conflicting interests

The author(s) declared no potential conflicts of interest with respect to the research, authorship, and/or publication of this article.

### Funding

The author(s) disclosed receipt of the following financial support for the research, authorship, and/or publication of this article: This work was supported by the grants from National Natural Science Foundation of China (81873995 and 81974334), The Preponderant Discipline Supporting Project of the Second Affiliated Hospital of Soochow University (XKTJ-XK202003), the Suzhou Special Foundation for the Key Diseases Diagnosis and Treatment(LCZX201904, LCZX201708), the Key Laboratory for Spinal Cord Injury Regeneration of Suzhou (SZS201807), and the Social Development Key Programs of Jiangsu Province—Advanced Clinical Technology (BE2019662,

BE2018656). This study was also supported by the Postgraduate Research & Practice Innovation Program of Jiangsu Province (KYCX19\_1983 and KYCX20\_2678). The Advanced Ph.D. research project of the Second Affiliated Hospital of Soochow University (SDFEYBS2011).

### ORCID iD

Xiaozhong Zhou  <https://orcid.org/0000-0003-0944-6570>

### Supplemental material

Supplemental material for this article is available online.

### References

- Liu J, Saul D, Boker KO, et al. Current methods for skeletal muscle tissue repair and regeneration. *Biomed Res Int* 2018; 2018: 1984879.
- Souza J and Gottfried C. Muscle injury: review of experimental models. *J Electromyogr Kinesiol* 2013; 23: 1253–1260.
- Chazaud B. Inflammation and skeletal muscle regeneration: leave it to the macrophages! *Trends Immunol* 2020; 41: 481–492.
- Jarvinen TA, Jarvinen TL, Kaariainen M, et al. Muscle injuries: biology and treatment. *Am J Sports Med* 2005; 33: 745–764.
- Smoak MM and Mikos AG. Advances in biomaterials for skeletal muscle engineering and obstacles still to overcome. *Mater Today Bio* 2020; 7: 100069.
- Tidball JG. Inflammatory processes in muscle injury and repair. *Am J Physiol Regul Integr Comp Physiol* 2005; 288: R345–R353.
- Smith C, Kruger MJ, Smith RM, et al. The inflammatory response to skeletal muscle injury: illuminating complexities. *Sports Med* 2008; 38: 947–969.
- Raimondo TM and Mooney DJ. Functional muscle recovery with nanoparticle-directed M2 macrophage polarization in mice. *Proc Natl Acad Sci U S A* 2018; 115: 10648–10653.
- Mantovani A, Biswas SK, Galdiero MR, et al. Macrophage plasticity and polarization in tissue repair and remodelling. *J Pathol* 2013; 229: 176–185.
- Tonkin J, Temmerman L, Sampson RD, et al. Monocyte/macrophage-derived IGF-1 orchestrates murine skeletal muscle regeneration and modulates autocrine polarization. *Mol Ther* 2015; 23: 1189–1200.
- Tidball JG. Regulation of muscle growth and regeneration by the immune system. *Nat Rev Immunol* 2017; 17: 165–178.
- Bai J, Zhang Y, Fan Q, et al. Reactive oxygen species-scavenging scaffold with rapamycin for treatment of intervertebral disk degeneration. *Adv Healthc Mater* 2020; 9: e1901186.
- Zheng X, Ding Z, Cheng W, et al. Microskin-inspired injectable MSC-laden hydrogels for scarless wound healing with hair follicles. *Adv Healthc Mater* 2020; 9: e2000041.
- Singer NG and Caplan AI. Mesenchymal stem cells: mechanisms of inflammation. *Annu Rev Pathol* 2011; 6: 457–478.
- Shi Y, Wang Y, Li Q, et al. Immunoregulatory mechanisms of mesenchymal stem and stromal cells in inflammatory diseases. *Nat Rev Nephrol* 2018; 14: 493–507.

16. Tajbakhsh S. Skeletal muscle stem cells in developmental versus regenerative myogenesis. *J Intern Med* 2009; 266: 372–389.
17. Borselli C, Storrie H, Benesch-Lee F, et al. Functional muscle regeneration with combined delivery of angiogenesis and myogenesis factors. *Proc Natl Acad Sci U S A* 2010; 107: 3287–3292.
18. Bai JY, Li Y, Xue GH, et al. Requirement of Galphai1 and Galphai3 in interleukin-4-induced signaling, macrophage M2 polarization and allergic asthma response. *Theranostics* 2021; 11: 4894–4909.
19. Zhang XY, Shan HJ, Zhang P, et al. LncRNA EPIC1 protects human osteoblasts from dexamethasone-induced cell death. *Biochem Biophys Res Commun* 2018; 503: 2255–2262.
20. Shabani M, Larizadeh MH, Parsania S, et al. Evaluation of destructive effects of exposure to cisplatin during developmental stage: no profound evidence for sex differences in impaired motor and memory performance. *Int J Neurosci* 2012; 122: 439–448.
21. Justice JN, Carter CS, Beck HJ, et al. Battery of behavioral tests in mice that models age-associated changes in human motor function. *Age* 2014; 36: 583–592.
22. Rivlin AS and Tator CH. Objective clinical assessment of motor function after experimental spinal cord injury in the rat. *J Neurosurg* 1977; 47: 577–581.
23. Ahmad M, Zakaria A and Almutairi KM. Effectiveness of minocycline and FK506 alone and in combination on enhanced behavioral and biochemical recovery from spinal cord injury in rats. *Pharmacol Biochem Behav* 2016; 145: 45–54.
24. Wang C, Wang J, Zhang X, et al. In situ formed reactive oxygen species-responsive scaffold with gemcitabine and checkpoint inhibitor for combination therapy. *Sci Transl Med* 2018; 10: eaan3682.
25. Kozakowska M, Pietraszek-Gremplewicz K, Jozkowicz A, et al. The role of oxidative stress in skeletal muscle injury and regeneration: focus on antioxidant enzymes. *J Muscle Res Cell Motil* 2015; 36: 377–393.
26. Valko M, Leibfritz D, Moncol J, et al. Free radicals and antioxidants in normal physiological functions and human disease. *Int J Biochem Cell Biol* 2007; 39: 44–84.
27. Beyfuss K and Hood DA. A systematic review of p53 regulation of oxidative stress in skeletal muscle. *Redox Rep* 2018; 23: 100–117.
28. Noctor G, Reichheld JP and Foyer CH. ROS-related redox regulation and signaling in plants. *Semin Cell Dev Biol* 2018; 80: 3–12.
29. Hemmings BA and Restuccia DF. PI3K-PKB/Akt pathway. *Cold Spring Harb Perspect Biol* 2012; 4: a011189.
30. Slomovitz BM and Coleman RL. The PI3K/AKT/mTOR pathway as a therapeutic target in endometrial cancer. *Clin Cancer Res* 2012; 18: 5856–5864.
31. Saxton RA and Sabatini DM. mTOR signaling in growth, metabolism, and disease. *Cell* 2017; 168: 960–976.
32. Wang LT, Ting CH, Yen ML, et al. Human mesenchymal stem cells (MSCs) for treatment towards immune- and inflammation-mediated diseases: review of current clinical trials. *J Biomed Sci* 2016; 23: 76.
33. Bernardo ME and Fibbe WE. Mesenchymal stromal cells: sensors and switchers of inflammation. *Cell Stem Cell* 2013; 13: 392–402.
34. Chamberlain CS, Clements AEB, Kink JA, et al. Extracellular vesicle-educated macrophages promote early achilles tendon healing. *Stem Cells* 2019; 37: 652–662.
35. Almalki SG and Agrawal DK. Key transcription factors in the differentiation of mesenchymal stem cells. *Differentiation* 2016; 92: 41–51.
36. Braun T and Arnold HH. Myf-5 and myoD genes are activated in distinct mesenchymal stem cells and determine different skeletal muscle cell lineages. *EMBO J* 1996; 15: 310–318.
37. Chio JCT, Wang J, Badner A, et al. The effects of human immunoglobulin G on enhancing tissue protection and neurobehavioral recovery after traumatic cervical spinal cord injury are mediated through the neurovascular unit. *J Neuroinflammation* 2019; 16: 141.
38. Pumberger M, Qazi TH, Ehrentraut MC, et al. Synthetic niche to modulate regenerative potential of MSCs and enhance skeletal muscle regeneration. *Biomaterials* 2016; 99: 95–108.
39. Xu Y, Fu M, Li Z, et al. A pro-survival and pro-angiogenic stem cell delivery system to promote ischemic limb regeneration. *Acta Biomater* 2016; 31: 99–113.
40. Denu RA and Hematti P. Effects of oxidative stress on mesenchymal stem cell biology. *Oxid Med Cell Longev* 2016; 2016: 2989076.
41. Quintero AJ, Wright VJ, Fu FH, et al. Stem cells for the treatment of skeletal muscle injury. *Clin Sports Med* 2009; 28: 1–11.
42. Grefte S, Kuijpers-Jagtman AM, Torensma R, et al. Skeletal muscle development and regeneration. *Stem Cells Dev* 2007; 16: 857–868.
43. Belcastro AN, Shewchuk LD and Raj DA. Exercise-induced muscle injury: a calpain hypothesis. *Mol Cell Biochem* 1998; 179: 135–145.
44. Charge SB and Rudnicki MA. Cellular and molecular regulation of muscle regeneration. *Physiol Rev* 2004; 84: 209–238.
45. Oishi Y and Manabe I. Macrophages in inflammation, repair and regeneration. *Int Immunol* 2018; 30: 511–528.
46. Waris G and Ahsan H. Reactive oxygen species: role in the development of cancer and various chronic conditions. *J Carcinog* 2006; 5: 14.
47. Phinney DG and Prockop DJ. Concise review: mesenchymal stem/multipotent stromal cells: the state of transdifferentiation and modes of tissue repair—current views. *Stem Cells* 2007; 25: 2896–2902.
48. Natsu K, Ochi M, Mochizuki Y, et al. Allogeneic bone marrow-derived mesenchymal stromal cells promote the regeneration of injured skeletal muscle without differentiation into myofibers. *Tissue Eng* 2004; 10: 1093–1112.
49. Kuznetsov SA, Krebsbach PH, Satomura K, et al. Single-colony derived strains of human marrow stromal fibroblasts form bone after transplantation in vivo. *J Bone Miner Res* 1997; 12: 1335–1347.
50. Choo KB, Tai L, Hymavathees KS, et al. Oxidative stress-induced premature senescence in Wharton's

- jelly-derived mesenchymal stem cells. *Int J Med Sci* 2014; 11: 1201–1207.
51. Kurtzeborn K, Kwon HN and Kuure S. MAPK/ERK signaling in regulation of renal differentiation. *Int J Mol Sci* 2019; 20: 1779.
  52. Huang Z, Wang X and Chen D. Signal proteins involved in myogenic stem cells differentiation. *Curr Protein Pept Sci* 2017; 18: 571–578.
  53. Zhang X, Wang L, Qiu K, et al. Dynamic membrane proteome of adipogenic and myogenic precursors in skeletal muscle highlights EPHA2 may promote myogenic differentiation through ERK signaling. *FASEB J* 2019; 33: 5495–5509.
  54. Yang W and Hu P. Skeletal muscle regeneration is modulated by inflammation. *J Orthop Translat* 2018; 13: 25–32.
  55. Ding DC, Shyu WC and Lin SZ. Mesenchymal stem cells. *Cell Transplant* 2011; 20: 5–14.